Comparative angle-resolved photoemission study of Ag nanometer films grown on fcc Fe(111) and bcc Fe(110)

Hiroyuki Sasaki,* Akinori Tanaka,† Shoji Suzuki, and Shigeru Sato‡
Department of Physics, Graduate School of Science, Tohoku University, Aoba-ku, Sendai 980-8578, Japan
(Received 8 March 2004; revised manuscript received 11 June 2004; published 23 September 2004)

A comparative study of the electronic structures of Ag nanometer films on pseudomorphic metastable fcc Fe(111) and bulklike bcc Fe(110) substrates has been carried out to investigate their quantized electronic structures. From low-energy electron diffraction and angle-resolved photoemission spectra, it has been confirmed that Ag nanofilms on both substrates grow in fcc [111] direction under optimized growth conditions. The photoemission spectra of both Ag nanofilms exhibit spectral features due to quantum-well (QW) states derived from the Ag *sp* valence electron. The nanofilm-thickness dependences of the binding energy of QW states are reproduced with calculated results based on a phase accumulation model. From the angle-resolved photoemission measurements, the effective mass of QW states along the direction parallel to the nanofilm surface were directly determined. From these results, we discuss the quantized electronic structures in Ag nanofilms grown on both bcc Fe and fcc Fe substrates.

DOI: 10.1103/PhysRevB.70.115415 PACS number(s): 73.21.Fg

I. INTRODUCTION

The physical properties of metallic nanostructures have attracted much interest because of various distinct physical properties due to quantum confinement effects. In particular, multilayers composed of alternating ferromagnetic and nonmagnetic metals show intriguing phenomena, such as giant magnetoresistance and oscillatory magnetic coupling.[1,2] From photoemission studies for the noble-metal nanofilms deposited on ferromagnetic transition-metal substrates, it has been reported that the spin-polarized quantum-well (QW) states in nonmagnetic layers mediate the exchange coupling between ferromagnetic layers.[3] In order to fully elucidate the coupling mechanism in these metallic multilayers, it is also indispensable to consider the detailed electronic coupling between nonmagnetic- and transition-metal layers. Photoemission and inverse photoemission spectroscopy have been used to study the quantum size effect on the electronic states in metallic nanofilms,[3–13] but to our knowledge, there is no report of a comparative study to date that highlights differences of QW states in noble-metal nanofilms on transition-metal substrates with different structures. Furthermore, most of these earlier studies were limited to noble-metal nanofilms deposited onto bulk (or bulklike) substrates. Bulk Fe undergoes a phase transition from a body centered cubic (bcc) phase to a face centered cubic (fcc) phase at 1184 K. On the other hand, the epitaxial growth of both bcc and fcc Fe films has been observed on Cu (100) and (111) clean surfaces.[14–18] From previous reports for the growth mode of Fe on Cu(111), Fe grows in the metastable fcc phase for the first several layers and transforms into the bulklike bcc phase for more deposition.[15–18] It has been also reported that the film morphology shows a complex dependence on growth temperature.[17] Therefore, we can control the structure of Fe substrates by varying their thickness and growth temperature. In the present work, we have prepared Ag nanofilms with various thicknesses on fcc and bcc Fe substrates and carried out angle-resolved photoemission measurements. From these results, we discuss the quantized electronic states in Ag nanofilms grown on these Fe substrates.

II. EXPERIMENT

The Ag nanofilms and Fe substrates were prepared by molecular beam epitaxy (MBE) using a JPS-100 (ANELVA Co. Ltd.) MBE system connected directly to an ARUPS 10 (VG Scientific Co. Ltd.) photoelectron spectrometer. The substrates used in the epitaxial growth were Si(111) single crystals. After a chemical treatment by Shiraki's method,[19] Si wafers were loaded into the ultrahigh vacuum (UHV) chamber. Si(111)-7×7 clean surfaces were obtained by annealing at 1150 K under UHV. First, a Cu(111) seed layer with a thickness of 30 nm was deposited onto a Si(111)-7×7 clean surface at room temperature and subsequently annealed at 450 K to enhance film uniformity. Next, Fe films with two different structures were deposited onto this Cu(111) seed layer. It has been reported that the metastable fcc phase transforms to the bulklike bcc Fe at the critical Fe thickness of about 0.5 nm on Cu(111) substrates at room temperature and this critical thickness increases with higher growth temperature.[17] We prepared the pseudomorphic fcc Fe(111) substrate using 0.8 nm-thickness deposition at 403 K, whereas a bcc Fe(110) substrate was obtained by 4.0 nm-thickness deposition at 90 K with subsequent annealing at 420 K. Finally, Ag nanofilms on these substrates were deposited at 90 K and subsequently annealed at 420 K. All the materials were evaporated from 3 kW electron-gun evaporators and all deposition rates were 0.005–0.01 nm/sec as monitored by calibrated quartz thickness monitors. The pressure during the deposition was kept in the 10^{-9} Pa range. The surface cleanliness and structure were checked by Auger electron spectroscopy and low-energy electron diffraction (LEED).

The thus-prepared samples were transferred into the photoemission chamber through the UHV chambers without exposure to air. Angle-resolved photoemission measurements

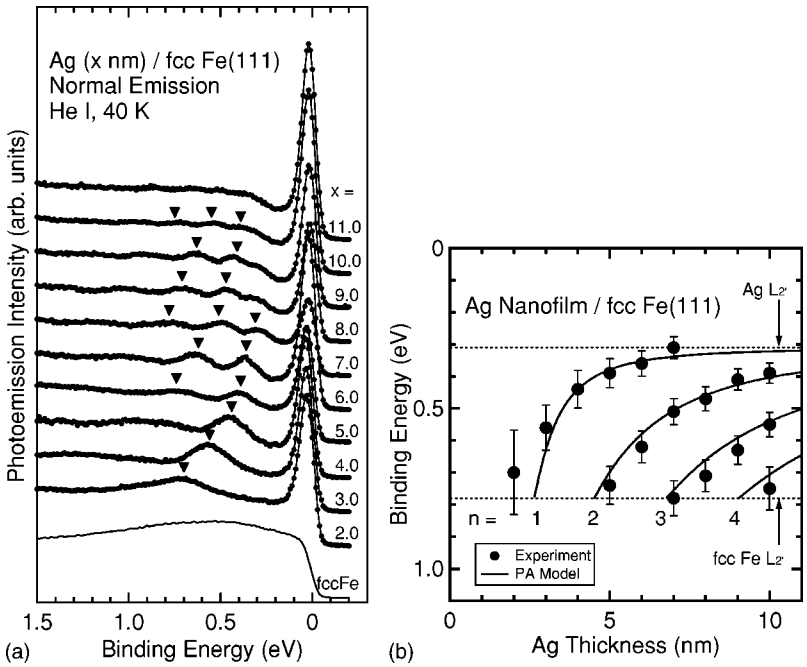

FIG. 1. (a) Angle-resolved photoemission spectra at normal emission geometry for Ag nanofilms with various thicknesses, grown on fcc Fe(111) substrate, excited by the He I ($h\nu$ =21.2 eV) resonance line at 40 K. Thickness of Ag nanofilms are indicated for each spectrum. (b) Nanofilm-thickness dependence of the binding energies of quantum-well (QW) states for Ag nanofilms grown on fcc Fe(111) substrate. Solid circles represent experimental data. Solid lines are the calculated results of QW states with n =1–3 by the phase accumulation (PA) model.

were performed with He I resonance line ($h\nu$=21.2 eV) as the excitation source. The base pressure of photoelectron spectrometer is in the 10^{-9} Pa range. The total energy and angular resolutions were about 65 meV and ±2.0°, respectively. All photoemission measurements were recorded at a sample temperature 40 K using a closed-cycle He refrigerator. The angle-resolved photoemission spectra showed no change in the course of the measurements.

III. RESULTS AND DISCUSSION

A. Ag(111) nanofilms grown on fcc Fe(111) substrate

Figure 1(a) shows angle-resolved photoemission spectra at normal emission geometry, measured for Ag nanofilms with various thicknesses grown on metastable fcc Fe(111) substrates. The spectrum for fcc Fe substrate is also shown. Brodde *et al.* have reported the photoemission spectra for a 5 ML-thick fcc Fe(111) film deposited onto a Cu(111) substrate.[18] These spectra are almost reproduced by the band calculation for fcc Fe.[20] The spectral features of the present fcc Fe(111) substrate are similar to this previous report[18] and quite different from those of bcc Fe(110) (Sec. III B.). Moreover, clear hexagonal LEED patterns are also observed. It is reconfirmed that the metastable fcc Fe(111) substrate has been obtained in this study. The spectrum for the Ag nanofilm with a thickness of 11 nm is almost identical with previously reported spectra for Ag(111) thick nanofilms[5,6,21,22] and for a bulk Ag(111) clean surface.[23,24] From these previous reports, the intense spectral feature just below the Fermi level is assigned to the well-known Shockley type surface state at the $\bar{\Gamma}$ symmetry point of the surface Brillouin zone (SBZ). The existence of this surface state, as well as a sharp LEED pattern, implies a good crystallinity. As shown in Fig. 1(a), the additional fine structures are observed at higher binding energy in the normal emission spectra for thinner nanofilms. As shown in Fig. 1(b), the binding energies of these spectral features shift to lower binding energies and the energy intervals between them decrease with increasing Ag nanofilm thickness. From the analogy to previous works for Ag(111) nanofilms grown on Cu(111) substrates,[6,21,22] it is concluded that these fine structures originate from QW states due to quantum confinement on Ag *sp* valence electrons. As shown in Fig. 1, the present QW states are observed in the binding-energy region between about 0.3 and 0.8 eV. The binding energy of the L edge of the Ag *sp* valence band is about 0.3 eV. Binding energy of 0.8 eV corresponds to the binding energy of the $L_{2'}$ point of fcc Fe.[20] Therefore, the Ag *sp* valence electrons are reflected at the Ag nanofilm/fcc Fe substrate interface because of the band mismatch along the direction normal to nanofilm surface. As shown in Fig. 1, the lowest binding-energy peaks converge to the L edge energy of the Ag *sp* valence band. This gives direct evidence that the QW states are derived from the Ag Λ_1 *sp* valence band.

In order to theoretically describe these experimental results, we have calculated the eigenvalues of QW states based on a phase accumulation (PA) model.[25,26] The quantization condition for the existence of the QW states is given by

$$2kd + \Phi_B + \Phi_C = 2n\pi, \tag{1}$$

where k is electron wave-vector component normal to the nanofilm surface, d is the nanofilm thickness, n is quantum number, and Φ_B and Φ_C are the phase shifts on the reflection of electron wave functions at nanofilm-vacuum and nanofilm-substrate interface, respectively. Here, k is determined by the energy dispersion of parental Ag *sp* valence band. The dispersion of Ag Λ_1 *sp* valence band along Γ-L direction based on the nearly free-electron two-band model is expressed by

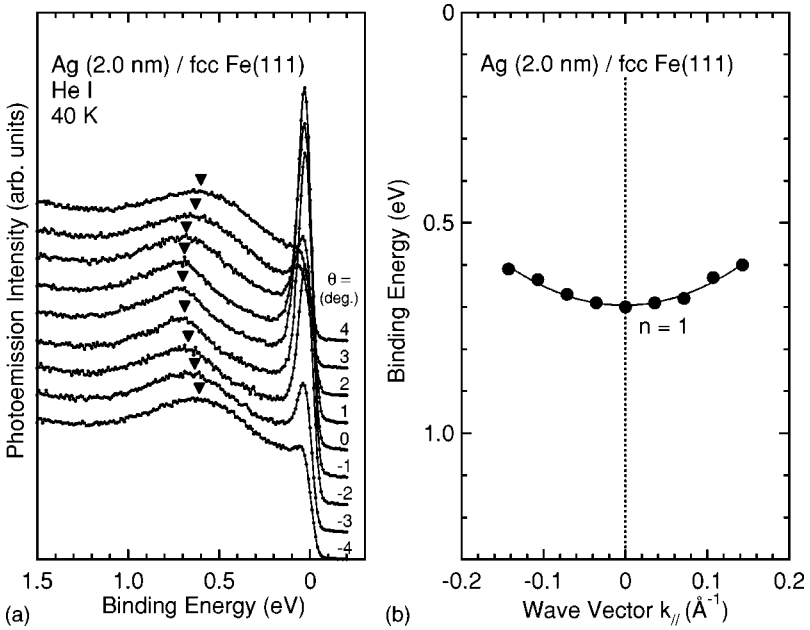

FIG. 2. (a) Angle-resolved photoemission spectra for the 2.0 nm-thick Ag nanofilm grown on fcc Fe(111) substrate. The polar emission angles with respect to the surface normal are indicated on each spectrum. (b) In-plane dispersion of the QW state in the Ag nanofilm with a thickness 2.0 nm. The solid line represents the result for the least-squares fit to experimental data.

$$k(E) = k_L - \sqrt{\frac{2m^*}{\hbar^2}}\sqrt{\frac{\hbar^2 k_L^2}{2m^*} + E - \sqrt{4\frac{\hbar^2 k_L^2}{2m^*}E + V_G^2}} \quad (2)$$

with $k_{\mathrm{L}}=1.33$ Å^{-1} is a wave vector at L point of Ag(111), $V_{\mathrm{G}}=2.08$ eV is the Fourier component of the crystal potential of Ag corresponding to a half of the hybridization gap, and $m^*=0.74m_{\mathrm{e}}$ is a effective mass of electrons in this valence band. The phase shift Φ_{B} on the reflection of electrons by the image potential at the Ag nanofilm surface is represented by

$$\Phi_B = \pi\left(\frac{3.4(\mathrm{eV})}{\sqrt{E_V - E}} - 1\right), \quad (3)$$

where $E_{\mathrm{V}}=E_{\mathrm{F}}+4.49$ eV is the vacuum level of the Ag(111) surface, using the WKB approximation.[27]

The Ag valence electrons in the present system are reflected by the mismatch of hybridization gaps between the Ag nanofilm and fcc Fe substrate at their interface. The phase shift Φ_{C} is determined by the relative energy position within the hybridization gap of the substrate, and is given by the empirical formula as follows:[26]

$$\Phi_{\mathrm{C}}(E) = 2\arcsin\left[\frac{E - E_{\mathrm{L}}}{E_{\mathrm{L}} - E_{\mathrm{U}}}\right]^{\frac{1}{2}} - \pi, \quad (4)$$

where $E_{\mathrm{L}}=0.79$ eV and $E_{\mathrm{U}}=-6.3$ eV are the binding energies of the lower and upper edge of the hybridization gap of the fcc Fe substrate from the band calculations.[20] The calculated results shown by solid lines in Fig. 1(b) mostly reproduce the experimental data. However, small deviations are found between experimental results and calculated ones especially for the thinner nanofilms. As discussed later, a possible reason for this deviation is related to electronic hybridization effects between the QW states and the electronic states in the substrate.

Figure 2(a) shows angle-resolved photoemission spectra measured for the Ag nanofilm with a thickness of 2 nm grown on a fcc Fe(111) substrate along the $\bar{\Gamma}-\bar{M}$ high symmetry line of SBZ, as excited by He I radiation at 40 K. From these spectra, it is found that the QW state with quantum number $n=1$ shift toward the Fermi level with increasing photoelectron emission angle. This indicates that the QW state has in-plane energy dispersion. We also plot the in-plane dispersions of this QW state in Fig. 2(b). The solid line in Fig. 2(b) is the result of a least-squares fit to each experimental data using parabolic function $E=E_0-2\hbar k_{\parallel}^2/2m_{\parallel}^*$, where E_0 and $m_{\parallel}^*$ are the binding energy at the $\bar{\Gamma}$ point and the in-plane effective mass, respectively. From this fit, we can derive the in-plane effective mass of QW state. We also carried out angle-resolved photoemission measurements along the $\bar{\Gamma}-\bar{K}$ high symmetry line. These dispersions are identical because parental Ag *sp* valence band is isotropic around the L point of BZ.

The in-plane effective masses of QW states are plotted as a function of nanofilm thickness in Fig. 3. In our previous study for the Ag(111)/Cu(111) system, the in-plane effective masses of QW states are about $m_{\parallel}^*/m_{\mathrm{e}}=0.35-0.45$ and are

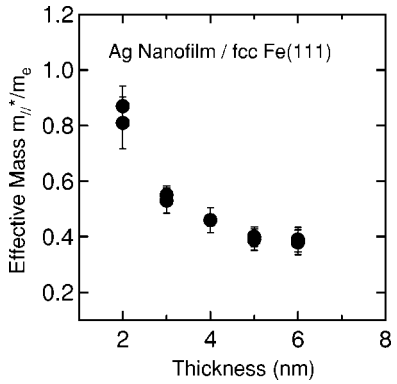

FIG. 3. The nanofilm-thickness dependence of in-plane effective mass of QW states obtained from least-squares fits to experimental data.

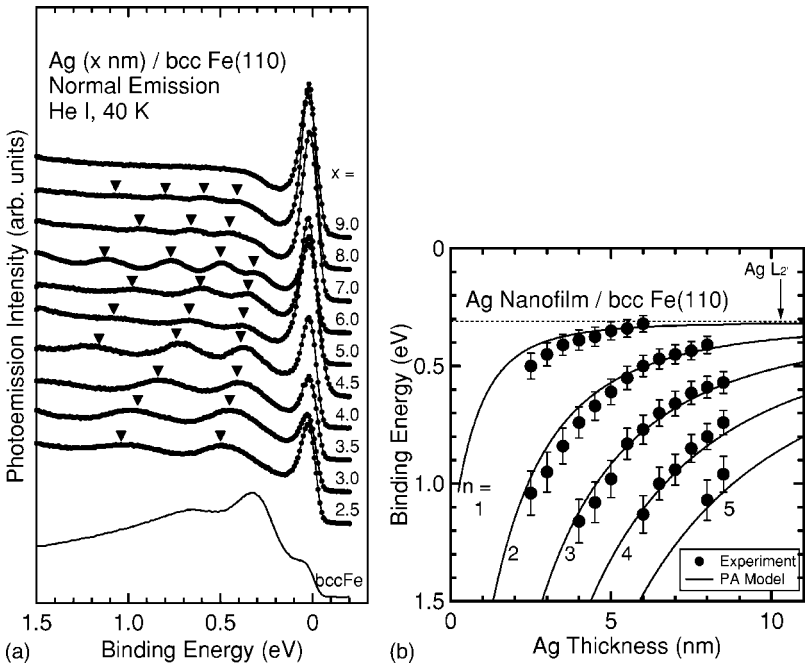

FIG. 4. (a) Angle-resolved photoemission spectra at normal emission geometry for Ag nanofilms with various thicknesses, grown on bcc Fe(110) substrate, excited by the He I $h\nu = 21.2$ eV resonance line at 40 K. Thickness of Ag nanofilms are indicated for each spectrum. (b) Nanofilm-thickness dependence of the binding energies of QW states for Ag nanofilms grown on bcc Fe(110) substrate. Solid circles represent experimental data. Solid lines are the calculated results of QW states with $n=1-5$ by the PA model.

identical with those of the parental bulk Ag *sp* valence band.[22] In this study, it is found that the in-plane effective mass of the QW states are identical with those in the Ag(111)/Cu(111) system for thicker (>4.0 nm) nanofilms. On the other hand, in-plane effective masses are enhanced for thinner nanofilms. For similar thickness, the binding energy of QW states also show deviation from the calculation using the PA model. One possible origin of the enhancement of in-plane effective mass is considered to originate from an in-plane confinement effect due to the finite domain size of nanofilms. However, the present Ag nanofilms exhibit the sharp LEED patterns. Furthermore, the photoemission intensity of the surface state decreases with increasing the photoelectron emission angle, indicating that the surface state on the present nanofilm surface disperses upward across the Fermi level with increasing the wave vector parallel to the surface similar to bulk Ag(111) surface.[28] Therefore, Ag nanofilms have sufficiently large domain size and such a three-dimensional confinement effect is considered to be negligible. Another possible candidate for such an effect is a hybridization effect with more localized states with larger effective mass. From the angle-resolved photoemission measurement for the present pseudomorphic fcc Fe(111) substrate, we confirmed that the Fe 3*d* derived valence band with a small dispersion exists in the binding energy region where the QW states are observed. Therefore, it is considered that this enhancement in the in-plane effective mass of QW state originates from a hybridization effect between the QW state in the Ag nanofilm and the 3*d*-derived electronic states in the fcc Fe substrate at their interface. Indeed, in our previous Ag(111)/Cu(111) system, where the hybridization effect between QW state and localized Cu 3*d*-state would be excluded, no enhancement of in-plane effective masses was observed even for thinner nanofilms. The nanofilm-thickness dependence of the in-plane effective masses would be reflected in the degree of hybridization effect with the electronic states of substrate.

The influence of the substrate electronic structure on the dispersion of quantized states in thinner nanofilms has been studied in the various systems.[7,8,10–13] The tight-binding analysis for the Cu/Co(100) system by Johnson *et al.*[7] has suggested that these hybridization effects are enhanced as the nanofilm becomes thinner. They also concluded that the enhancements of in-plane effective masses originated from interfacial hybridization effects between QW states and the substrate. These theoretical approaches would be necessary in order to analyze the present nanofilm-thickness dependence of the in-plane effective masses quantitatively.

B. Ag(111) nanofilms grown on a bcc Fe(110) substrate

Figure 4(a) shows angle-resolved photoemission spectra at normal emission geometry for Ag nanofilms of various thicknesses grown on bcc Fe(110) substrates. The spectrum for bcc Fe(110) substrate is very similar to that for bulk bcc Fe(110) surface.[29] Clear LEED images similar to previous report[16] are also observed. Therefore, it is considered that the bulklike bcc Fe(110) substrate is obtained. In the spectra for Ag nanofilms, the features derived from the Shockley surface state are also observed. It is confirmed again that the Ag nanofilm grow on the bcc Fe(110) substrate in the [111] direction according to well-known Nishiyama-Wassermann epitaxial relationship.[30] Similar to the Ag(111)/fcc Fe(111) system, the fine structures derived from the QW states are also observed. Figure 4(b) shows the nanofilm-thickness dependence of the binding energy of QW states. We also calculated the eigenvalues of QW states in the present Ag(111)/bcc Fe(110) system by the PA model as described above. However, the quantum confinement regime is slightly different from the Ag(111)/fcc Fe(111) system. In the fcc Ag(111)/fcc Fe(111) system, the symmetries of electronic states in the nanofilm and substrate along the normal direction are identical. Even for fcc(100)-phase nanofilms on transition-metal bcc(100)-phase substrates, such as

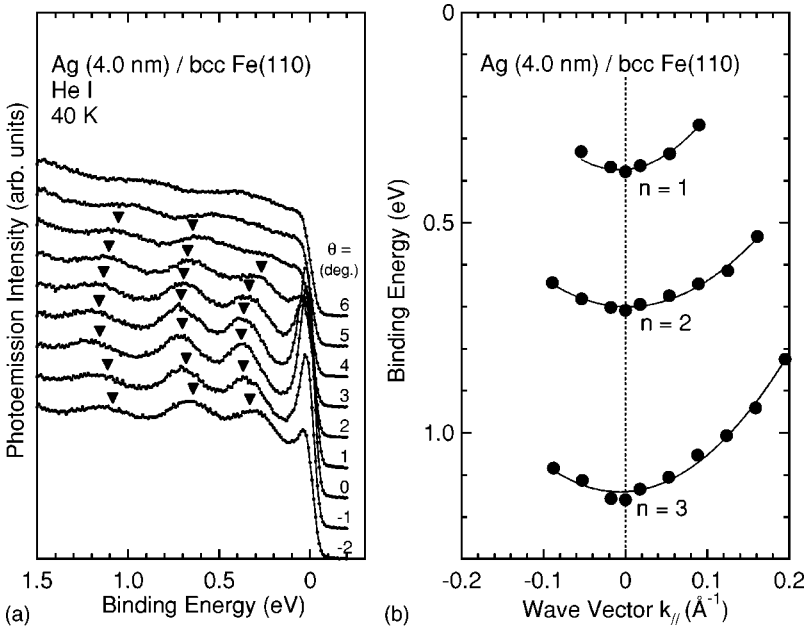

FIG. 5. (a) Angle-resolved photoemission spectra for the 4.0 nm-thick Ag nanofilm grown on bcc Fe(110) substrates. The polar emission angles with respect to the surface normal are indicated on each spectrum. (b) In-plane dispersion of the QW states in the Ag nanofilm with a thickness 4.0 nm. The solid lines represent the results for the least-squares fits to experimental data.

Ag(100)/bcc Fe(100) (Ref. 9) and Ag(100)/V(100) systems,[8] the physical situations are similar, and their electronic states have the identical symmetry (Δ symmetry). In the present system, however, the growth directions of the Ag nanofilm and the Fe substrate are fcc[111] and bcc[110] and this leads to the different symmetries of electronic states; namely, Λ and Σ symmetry, respectively. Furthermore, it has been reported that Ag(111) and bcc Fe(110) have a large anisotropic lattice mismatch.[30] It is considered that the Ag valence electron is mostly reflected at the Ag-bcc Fe interface due to the completely different symmetries of the electronic states along the normal direction. This situation would lead to a simple assumption, the phase shift $\Phi_C = -\pi$ at all binding energies. The solid lines of Fig 4(b) are the results obtained from Eq. (1) and reproduce the experimental data well. From these results, it is considered that Ag *sp* valence electrons are reflected almost completely at the nanofilm-substrate interface due to the difference of the symmetries of the electronic states.

Figure 5(a) shows angle-resolved photoemission spectra measured for the Ag nanofilm with a thickness of 4.0 nm grown on a bulklike bcc Fe(110) substrate along the $\bar{\Gamma}-\bar{M}$ high symmetry line, excited by He I radiation at 40 K. In the same way as the Ag(111)/fcc Fe(111) system, we obtained the in-plane effective masses of QW states from least-square fits [Fig. 5(b)]. We plot the in-plane effective mass as a function of the binding energy at $\bar{\Gamma}$ point in Fig. 6. It is found that the dependence of the in-plane effective mass on the binding energy is mostly consistent with that derived from the bulk band calculation[31] (shown as a solid line in Fig. 6.) and seems to be independent of the nanofilm thickness. This means that the in-plane effective masses of QW states are equivalent to those of the parental valence bands, although 3*d* electron bands with much larger effective mass also exist in the Fe substrate in the binding-energy region where the QW states are observed. In the Ag(111)/fcc Fe(111) system (Sec. III A.), the QW states in nanofilm hybridize with electronic structure of substrate for thinner nanofilms because the both nanofilm and substrate have the same symmetry of their electronic states. In contrast, the crystalline structures of nanofilm and substrate are different in Ag(111)/bcc Fe(110) system, leading to different symmetries of the electronic states. Therefore, it is considered that the electronic coupling between the QW states and the electronic states of substrates is quite small. Consequently, in-plane effective masses of QW states are not enhanced from those of Ag bulk band even for thinner nanofilms. As discussed above, the calculation using the PA model taking into account this "hard wall at interface" assumption also reproduces the experimental results. Therefore, it would be also indispensable to take account into their physical structures in order to discuss such a hybridization effect between QW states in nanofilms and electronic states of substrates.

IV. SUMMARY

A comparative angle-resolved photoemission study for Ag nanofilms on pseudomorphic metastable fcc Fe(111) and bcc

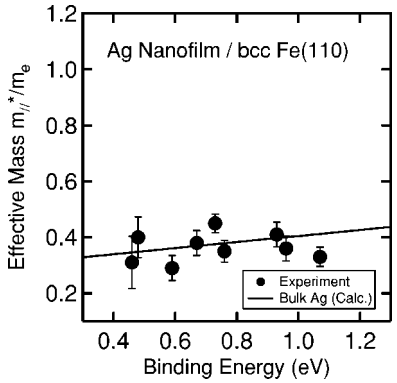

FIG. 6. In-plane effective mass of QW state as a function of the binding energy at $\bar{\Gamma}$ point. The solid line represents calculated results for bulk Ag (Ref. 31).

Fe(110) substrates has been carried out in order to investigate their quantized electronic structures. From angle-resolved photoemission measurements for various nanofilm thicknesses, we observe fine structures originating from quantum-well (QW) states of Ag *sp* valence electrons. We analyzed the binding- energy dependence of these QW states on nanofilm thickness by calculations based on the phase accumulation model especially taking into account differences in the phase shifts at the Ag-Fe interface. From detailed angle-resolved photoemission measurements, it is found that in the Ag(111)/fcc Fe(111) system the in-plane effective mass of QW states are enhanced especially for thinner nanofilms. It is concluded that this enhancement of in-plane effective mass is originated from the electronic hybridization effect between QW states in Ag nanofilm and 3*d*-derived electronic states in the fcc Fe(111) substrate. On the other hand, in the Ag(111)/bcc Fe(110) system, the in-plane effective masses are almost identical with those in bulk Ag, although 3*d* bands of the Fe substrate with larger effective masses exist in the energy region where the QW states are observed. It is considered that the electrons in nanofilm are completely reflected at nanofilm-substrate interface because their crystalline structures (leading to the symmetries of electronic states) are different. From these results, it is concluded that it is essential to take into account not only the electronic structures of substrates but also their physical structures in order to discuss QW states in nanofilms.

ACKNOWLEDGMENTS

This work was supported by grants from the Ministry of Education, Culture, Sports, Science and Technology of Japan and Cooperative Research Program of the Center for Interdisciplinary Research of Tohoku University. H.S. thanks the Japan Society for Promotion of Science (JSPS) for financial support.

*Present address: Nanomaterials Laboratory, National Institute for Materials Science (NIMS), 1-1, Namiki, Tsukuba 305-0044, Japan.

†Present address: Department of Mechanical Engineering, Faculty of Engineering, Kobe University, 1-1, Rokkodai, Nada-ku, Kobe 657-8501, Japan.

‡Present address: Department of Electronics, Tohuku Institute of Technology, 6 Futatsusawa, Taihaku-ku, Sendai 982-8588, Japan.

[1] M. N. Baibich, J. M. Broto, A. Fert, F. Nguyen Van Dau, F. Petroff, P. Etienne, G. Creuzet, A. Friederich, and J. Chazelas, Phys. Rev. Lett. **61**, 2472 (1988).

[2] S. S. P. Parkin, Phys. Rev. Lett. **67**, 3598 (1991).

[3] J. E. Ortega and F. J. Himpsel, Phys. Rev. Lett. **69**, 844 (1992).

[4] T.-C. Chiang, Surf. Sci. Rep. **39**, 183 (2000), and references therein.

[5] T. Miller, A. Samsavar, G. E. Franklin, and T.-C. Chiang, Phys. Rev. Lett. **61**, 1404 (1988).

[6] M. A. Mueller, T. Miller, and T.-C. Chiang, Phys. Rev. B **41**, 5214 (1990).

[7] P. D. Johnson, K. Garrison, Q. Dong, N. V. Smith, D. Li, J. Mattson, J. Pearson, and S. D. Bader, Phys. Rev. B **50**, 8954 (1994).

[8] T. Valla, P. Pervan, M. Milun, A. B. Hayden, and D. P. Woodruff, Phys. Rev. B **54**, 11 786 (1996).

[9] J. J. Paggel, T. Miller, and T.-C. Chiang, Science **283** 1709 (1999).

[10] A. Tanaka, H. Sasaki, K. Takahashi, W. Gondo, S. Suzuki, and S. Sato, J. Phys. Chem. Solids **60**, 1995 (1999).

[11] A. M. Shikin, O. Rader, G. V. Prudnikova, V. K. Adamchuk, and W. Gudat, Phys. Rev. B **65**, 075403 (2002).

[12] L. Aballe, C. Rogero, P. Kratzer, S. Gokhale, and K. Horn, Phys. Rev. Lett. **87**, 156801 (2001).

[13] A. Danese and R. A. Bartynski, Phys. Rev. B **65**, 174419 (2002).

[14] M. Wuttig, B. Feldmann, and T. Flores, Surf. Sci. **331–333**, 659 (1995).

[15] Y. Ando and D. J. Dingley, Jpn. J. Appl. Phys., Part 1 **29**, 939 (1990).

[16] D. Tian, F. Jona, and P. M. Marcus, Phys. Rev. B **45**, 11 216 (1992).

[17] M. T. Kief and W. F. Egelhoff, Jr., J. Vac. Sci. Technol. A **11**, 1661 (1993).

[18] A. Brodde, K. Dreps, J. Binder, C. Lunau, and H. Neddermeyer, Phys. Rev. B **47**, 6609 (1993).

[19] A. Ishizaka and Y. Shiraki, J. Electrochem. Soc. **133**, 666 (1986).

[20] D. Bagayoko and J. Callaway, Phys. Rev. B **28**, 5419 (1983); D. Bagayoko (private communication).

[21] A. Tanaka, K. Takahashi, M. Hatano, K. Tamura, S. Suzuki, and S. Sato, J. Surf. Anal. **3**, 468 (1997).

[22] K. Takahashi, A. Tanaka, M. Hatano, H. Sasaki, S. Suzuki, and S. Sato, J. Electron Spectrosc. Relat. Phenom. **88–91**, 347 (1998).

[23] A. P. Shapiro, A. L. Wachs, and T.-C. Chiang, Solid State Commun. **58**, 121 (1986).

[24] S. D. Kevan and R. H. Gaylord, Phys. Rev. B **36**, 5809 (1987).

[25] N. V. Smith, Phys. Rev. B **32**, 3549 (1985).

[26] N. V. Smith, N. B. Brookes, Y. Chang, and P. D. Johnson, Phys. Rev. B **49**, 332 (1994).

[27] E. G. McRae and M. L. Kane, Surf. Sci. **108**, 435 (1981).

[28] R. Paniago, R. Matzdorf, G. Meister, and A. Goldmann, Surf. Sci. **336**, 113 (1995).

[29] A. M. Turner and J. L. Erskine, Phys. Rev. B **25**, 1983 (1982).

[30] T. Furukawa and K. Koike, Phys. Rev. B **57**, 2694 (1998).

[31] K.-M. Ho, C.-L. Fu, S. H. Liu, D. M. Kolb, and G. Paizza, J. Electroanal. Chem. Interfacial Electrochem. **150**, 235 (1983).